Multiple-State Equilibrium Unfolding of Guanidino Kinases†

Martin Gross,*,‡,⊥ Ariel Lustig,§ Theo Wallimann,‡,# and Rolf Furter‡,||

Institute for Cell Biology, Swiss Federal Institute of Technology, ETH-Hönggerberg, CH-8093 Zürich, Switzerland, and Department of Biophysical Chemistry, Biocenter, University of Basel, CH-4056 Basel, Switzerland

Received March 13, 1995; Revised Manuscript Received May 23, 1995⊗

ABSTRACT: The denaturant-induced equilibrium unfolding of octameric mitochondrial creatine kinase, dimeric cytosolic muscle-type creatine kinase, and monomeric arginine kinase was investigated. Stable unfolding intermediates for all three enzymes were manifested by a strongly biphasic red shift of intrinsic protein fluorescence upon increasing denaturant concentrations. In the intermediate state, all proteins were monomeric and enzymatically inactive, but still retained a globular shape. Native tertiary structure interactions were largely disrupted, while at least 50% of the secondary structures were conserved, as suggested by near- and far-UV circular dichroism, respectively. A significantly increased surface hydrophobicity of the intermediate conformation, compared to both the native and the fully unfolded states, was observed by the binding of the hydrophobic fluorescent dye ANS. The observed properties agree formally with the definition of the molten globule state, but can be alternatively explained by a sequential unfolding of individual domains, involving a transient exposure of domain interfaces. Very similar unfolding profiles for all three proteins suggest that the formation of stable unfolding intermediates is not a consequence of the specific oligomeric structures of the CKs but rather due to a common, probably two-domain architecture of the guanidino kinase protomers.

Studies on the equilibrium unfolding of globular proteins provide insight into the hierarchy of structural levels that governs both the conformational stability and the folding/unfolding pathways of proteins. Lately, the concept of the molten globule (MG)[1] (Kuwajima, 1989) has attracted considerable attention and stimulated a large number of equilibrium denaturation studies, since MG-type structures appear to be relevant as kinetic intermediates during the folding process of proteins both *in vitro* (Ptitsyn et al., 1990) and *in vivo* (Martin et al., 1991). However, most proteins for which equilibrium intermediates have been thoroughly characterized are small monomeric, single-domain proteins; up to now only a few larger proteins, such as multidomain and oligomeric proteins, have been studied (Herold & Kirschner, 1990; Missiakas et al., 1990). Such proteins are of particular interest since their equilibrium unfolding behavior can yield additional insight into the relative stability and folding autonomy of individual domains, as well as into the interdependence of folding and oligomerization processes.

The guanidino kinases (ATP:guanidinophosphotransferases) represent an enzyme family with closely related primary sequences and large structural similarities (Oriol & Landon, 1970; Roustan et al., 1970; Mühlebach et al., 1994). Lobster arginine kinase (ArgK) is a monomer of 40 kDa, while the cytosolic isoforms of creatine kinase (CK) are found exclusively as dimers of 86 kDa, and the mitochondrial CK isoforms (Mi-CK) even form 340-kDa octamers that can be readily dissociated into dimers *in vitro* (Schlegel et al., 1988; Gross & Wallimann, 1993, 1995). Although no high-resolution crystal structure of any guanidino kinase has been published yet, it has been postulated from biochemical and biophysical evidence that the protomer of these enzymes is composed of two globular, flexibly linked domains (Dumas & Janin, 1983; Morris & Cartwright, 1990).

Several investigations on the denaturant-induced unfolding and refolding of CK were undertaken previously. Some of these studies focused on the question of whether the monomeric CK subunit is enzymatically active (Bickerstaff et al., 1980; Grossman et al., 1981, 1986; Price & Stevens, 1982; Grossman, 1984), while others compared the denaturation behavior of the enzyme's active site to the global unfolding of the protein (Yao et al., 1984; Zhou & Tsou, 1985). Our recent investigation on the role of Trp residues in the octameric chicken Mi-CK used fluorescence-monitored quanidine hydrochloride (GdnHCl) equilibrium unfolding as an assay for conformational stability. There, we found preliminary evidence that Mi-CK denatures via some stable intermediate (Gross et al., 1994). In the present study, we have followed up this observation, and we have additionally analyzed rabbit M-CK and lobster ArgK to study the interdependence of subunit dissociation and unfolding processes and to reveal features that might be common to the entire family of guanidino kinases. To resolve as many details of the unfolding process as possible, a large variety

† This work was supported by grants from the Helmut-Horten-Stiftung and the Swiss National Science Foundation (SNF Grant 31-33907.92 to T.W. and R.F.).

* To whom correspondence should be addressed.

‡ Swiss Federal Institute of Technology.

§ University of Basel.

|| Current address: Dept. of Biochemistry and Molecular Biology, Lederle Graduate Research Center, University of Massachusetts, Amherst MA 01003.

⊥ Current address (from Aug 1, 1995): MRC Unit for Protein Function and Design, Cambridge University Chemical Department, Lensfield Rd., Cambridge CB2 1EW, U.K. Fax: +44-1223-336445.

Reprint requests should be addressed to T.W., ETH Zürich.

⊗ Abstract published in *Advance ACS Abstracts,* July 15, 1995.

[1] Abbreviations: ANS, 8-anilinonaphthalene-1-sulfonic acid; ArgK, arginine kinase; BSA, bovine serum albumin; buffer A, 100 mM sodium phosphate, 5 mM 2-ME, and 0.1 mM EDTA, pH 7.4; CK, creatine kinase; DTT, dithiothreitol; EDTA, ethylenediaminetetraacetic acid; GdnHCl, guanidine hydrochloride; I, intermediate folding state; 2-ME, 2-mercaptoethanol; MG, molten globule; Mi-CK, mitochondrial creatine kinase; Mi_b-CK, chicken sarcomeric mitochondrial creatine kinase; N, native state; OPTA, *o*-phthalic anhydride; 3-PGK, 3-phosphoglycerate kinase; SEC-FPLC, size-exclusion fast protein liquid chromatography; U, (fully) unfolded state.

0006-2960/95/0434-10350$09.00/0

of parameters, including enzyme activity, Trp fluorescence, near- and far-UV circular dichroism (CD), hydrophobic surface exposure [anilinonaphthalenesulfonic acid (ANS) binding], and hydrodynamic properties (size-exclusion FPLC, analytical ultracentrifugation) were measured. Our results indicate the occurrence of stable folding intermediates, the formation of which might be related to the supposed two-domain structure of the guanidino kinases.

MATERIALS AND METHODS

Protein Sources. Chicken sarcomeric mitochondrial creatine kinase (Mi_b-CK) was isolated from the *Escherichia coli* strain BL21(DE3)pLysS transformed with the expression vector pRF23 as described (Furter et al., 1992). Rabbit muscle creatine kinase (M-CK) and lobster tail arginine kinase (ArgK) were products of Boehringer (Mannheim) and Sigma, respectively; all protein preparations were homogeneous as judged by Coomassie-stained SDS−polyacrylamide gels. Protein concentrations were determined with the Bio-Rad dye adsorption assay (Bradford, 1976), using BSA as standard.

Guanidine Hydrochloride and Urea Denaturation Series. All denaturation experiments were performed in buffer A (100 mM sodium phosphate, pH 7.4, 5 mM 2-ME, and 0.1 mM EDTA), unless stated otherwise. Concentrated stock solutions of GdnHCl and urea (UltraPure, ICN) were prepared in buffer A and adjusted to pH 7.4. Protein samples were incubated at defined denaturant concentrations in buffer A overnight (≥18 h) at 22 °C to achieve equilibrium. For fluorescence spectroscopy and enzyme activity measurements, the samples were denatured at a protein concentration of 25 μg/mL, unless stated otherwise; for CD spectroscopy, SEC-FPLC, and analytical ultracentrifugation, the denaturations were carried out at higher protein concentrations up to 0.5 mg/mL.

Determination of Enzyme Activity. CK and ArgK enzyme activities were determined by the pH stat assay as described (Wallimann et al., 1984), monitoring the amount of protons consumed or produced by the enzymatic reaction. The CK reaction was measured in the reverse direction (ATP production) at pH 7.0, with the assay solution containing 10 mM phosphocreatine, 4 mM ADP, 10 mM $MgCl_2$, 60 mM KCl, 0.1 mM EGTA, and 1 mM 2-ME. ArgK activity was determined in the forward direction (phosphoarginine production) at pH 8.0; the assay mix contained 2 mM arginine, 8.3 mM ATP, 9.3 mM $MgCl_2$, and 1 mM 2-ME. Importantly, the residual denaturant concentration in the assay mix was adjusted uniformly to 0.05 M GdnHCl or urea. Otherwise, the denaturation curves would have been significantly distorted by inhibitory effects exerted by the denaturants (see also Discussion).

Size-Exclusion Chromatography (SEC-FPLC). For the determination of molecular size at equilibrium, SEC experiments were performed at 4 °C on a HR 30/10 Superose-12 FPLC column (Pharmacia), using the respective denaturation buffers as the eluent. The flow rate was set at 0.5−0.7 mL/min, such that complete elution of the protein samples took about 20 min. To assess the oligomeric state of the denatured proteins, samples were "globularized" (see Results) by dilution to a final concentration of 0.3 M GdnHCl and to a protein concentration of ≤40 μg/mL. The diluted samples were immediately applied to the SEC-FPLC column equilibrated in 0.3 M GdnHCl. The column was calibrated using the set of globular reference proteins provided by Pharmacia.

Fluorescence Spectroscopy. Fluorescence emission spectra were recorded on a SPEX Fluorolog-2 instrument, equipped with a 450-W xenon arc lamp as excitation source. All data were acquired in the ratio mode, using a rhodamine-B reference quantum counter, and spectra were corrected for variations in the responses of the emission gratings and the photomultiplier. Quartz cells (1 cm) were placed in a thermostated sample holder, and fluorescence emission was measured at 20 °C with rectangular excitation. For measurements of intrinsic protein fluorescence, the excitation wavelength was set at 280 nm, and emission spectra were recorded between 300 and 420 nm. To obtain denaturation profiles suitable for quantitative evaluation, the changes in protein fluorescence were plotted as intensity-weighted average emission wavelength (Royer et al., 1993),

$$\langle\lambda\rangle = \sum\lambda_i F_i / \sum F_i$$

versus denaturant concentration. λ_i and F_i represent the wavelengths measured and the corresponding emission intensities, respectively.

ANS Binding Assay. Samples from GdnHCl denaturation series were assayed for hydrophobic surface exposure by incubation with a 50-fold molar excess of anilinonaphthalenesulfonic acid (ANS) for ≥30 min at 22 °C in the dark, followed by measuring fluorescence emission spectra with excitation at 350 nm. Appropriate blank spectra of ANS in the corresponding denaturation buffers were subtracted to obtain the net fluorescence enhancement caused by dye adsorption to the protein.

CD Spectroscopy. CD spectra were measured at 22 °C on a Jasco J-710 dichrograph, using cylindrical 0.02-cm and 1-cm quartz cells for far- and near-UV CD spectra, respectively. After subtracting appropriate buffer blanks, mean residue ellipticities were calculated, using the mean amino acid M_r of 113.4, calculated from the protein sequence of Mi_b-CK.

Analytical Ultracentrifugation. Sedimentation velocity and sedimentation equilibrium runs were performed at 20 °C in a Beckman XLA analytical ultracentrifuge, equipped with a UV absorbance detection system. Double-sector, 12-mm, Kel-F and charcoal cells were used for sedimentation velocity and sedimentation equilibrium experiments, respectively. To the samples denatured at 1 M GdnHCl was freshly added 15 mM DTT prior to the centrifugation runs in order to reduce intermolecular disulfide bonds. Sedimentation coefficients ($s_{20,w}$) were calculated from plots of ln r *vs* t (r representing the boundary position at time t) and corrected for the densities and viscosities of the solutions. Average molecular weights (M_r) were calculated from the sedimentation equilibrium profiles with the program XLAEQ (Beckman), assuming a partial specific volume of 0.73 cm^3/g for the protein. The homogeneity of molecular weights was tested by repeating the M_r calculations after successively truncating the data sets from the meniscus and from the cell bottom, respectively. Systematic variations of the average M_r upon truncation were taken as an indication of polydispersity (Cantor & Schimmel, 1980).

Quantitative Analysis of Unfolding Profiles. According to Pace (1986), a linear relationship between the denaturant concentration [D] and the free energy of any A → B unfolding transition was assumed,

$$\Delta G_{ab} = \Delta G_{0,ab} - m_{ab}[D] \quad (1)$$

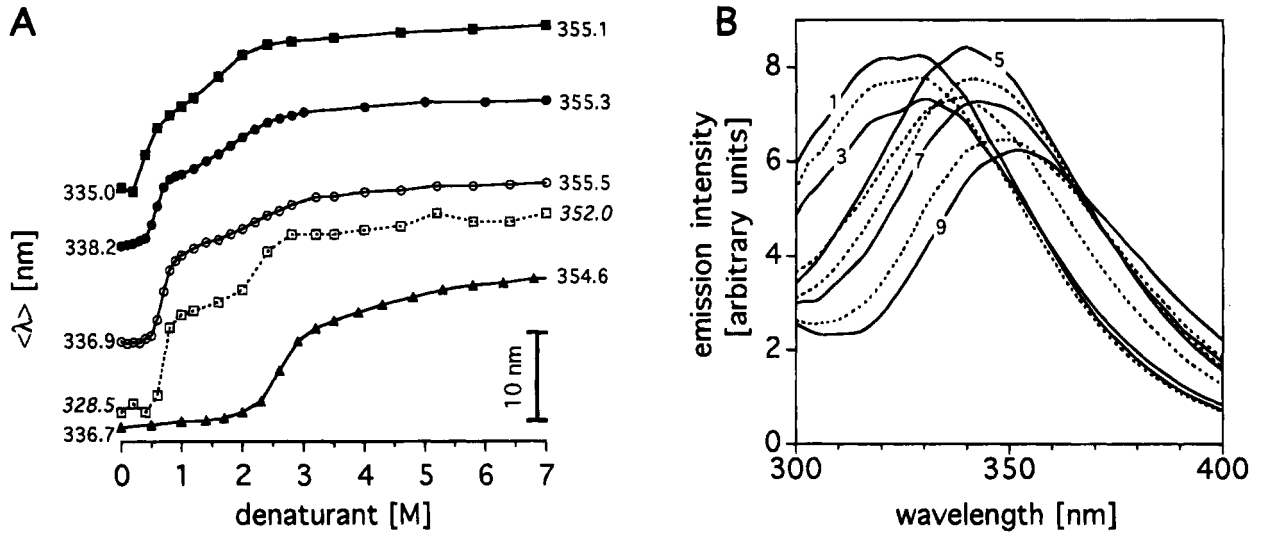

FIGURE 1: Changes in protein fluorescence upon equilibrium unfolding. (A) Fluorescence unfolding profiles. Mi-CK, M-CK, and ArgK (25 μg/mL) were denatured overnight at 22 °C in buffer A containing the indicated concentrations of GdnHCl or urea. Intensity-weighted average emission wavelengths ($\langle\lambda\rangle$) were calculated from intrinsic fluorescence emission spectra recorded from 300 to 420 nm, with excitation at 280 nm. $\langle\lambda\rangle$ profiles are presented for Mi-CK (GdnHCl), ○; M-CK (GdnHCl), ●; ArgK (GdnHCl), ■; and Mi-CK (urea), ▲. For comparison, the λ_{max} profile for Mi-CK (GdnHCl), □, is shown. Initial and final $\langle\lambda\rangle$ values are indicated in the plot; λ_{max} values are given in italics. (B) Fluorescence emission spectra of Mi-CK at selected GdnHCl concentrations. The spectra are alternatingly presented as solid and dashed lines, odd spectra numbers are indicated. 1, no denaturant; 2, 0.4 M; 3, 0.6 M; 4, 0.8 M; 5, 1.0 M; 6, 1.6 M; 7, 2.0 M; 8, 2.8 M; 9, 8.0 M GdnHCl.

with an intercept ($\Delta G_{0,ab}$) corresponding to the free energy of unfolding at zero denaturant concentration and a slope (m_{ab}) that reflects the cooperativity of the transition ("cooperativity index"). For a three-state unfolding process (N ⇌ I ⇌ U), including an intermediate state I, the observed fractional signal change, f_{app}, can be assumed to be additively composed of the individual contributions of the two transitions,

$$f_{app} = \alpha_{ni} f_{ni} + (1 - \alpha_{ni}) f_{ia} \qquad (2)$$

α_{ni} representing the fractional contribution of the N → I transition to the total signal change. The values for f_{ni} and f_{iu} were substituted by denaturant-dependent terms derived from eq 1, yielding an expression that could be fit to the experimental denaturation profiles:

$$f_{app} = \frac{\alpha K_{ni}}{1 + K_{ni}} + \frac{(1 - \alpha) K_{iu}}{1 + K_{iu}} \qquad (3)$$

with the equilibrium constants $K_{ab} = \exp((m_{ab}[D] - \Delta G_{0,ab})/RT)$ for each transition.

Since the fitting of eq 3 to the experimental curves of f_{app} vs [D] required the floating of five unknown parameters (α_{ni}, $\Delta G_{0,ni}$, $\Delta G_{0,iu}$, m_{ni}, m_{iu}), good initial estimates of these values were needed. Such preliminary values could easily be obtained by fitting a simple two-state model to the first part (transition N → I) of the biphasic denaturation curves or to an independent experimental parameter that only measured the N → I transition, such as enzyme activity. The calculated N → I transition curve was then subtracted from the complete denaturation profile, such that an approximate I → U curve was obtained. This curve was again fit to a two-state model. The values for α_{ni}, $\Delta G_{0,ni}$, $\Delta G_{0,iu}$, m_{ni}, and m_{iu} obtained from the two preliminary fits were then used as starting values for the final least-squares fitting of eq 3 to the original denaturation profile.

To simplify the analysis and to compare the denaturation behavior of the three proteins with different quaternary structures, all denaturation profiles were treated according to this unimolecular three-state model. All calculations were performed on an Apple Macintosh computer, using the program KaleidaGraph.

RESULTS

Equilibrium Unfolding of Guanidino Kinases; Involvement of a Stable Intermediate Species: Changes in Protein Fluorescence. The GdnHCl-induced equilibrium unfolding of all three guanidino kinases studied (Mi-CK, M-CK, ArgK) exhibited a strongly biphasic profile when monitored by the red shift of intrinsic protein fluorescence (using $\langle\lambda\rangle$ values, Figure 1A), indicating that the transition from the native (N) to the fully unfolded (U) state involves a stable intermediate species (I). The highly cooperative N → I transition (at 0.7, 0.6, and 0.4 M GdnHCl for Mi-CK, M-CK, and ArgK, respectively) resulted in a red shift by ≥10 nm of the fluorescence emission maximum and of the average emission wavelength (Figure 1A). For all three proteins, the emission maximum of the I state was uniformly positioned at 339.5 ± 0.5 nm, irrespective of the distinct maximum wavelengths in the native state, which were 328.5, 330, and 319 nm for Mi-CK, M-CK, and ArgK, respectively. Such a uniform maximum position was also found for the I state of all Trp single mutants of Mi-CK (Gross et al., 1994). These observations suggest that, in the I state, all Trp residues (five in wild-type Mi-CK, four in M-CK, two in ArgK) are in a similar, moderately hydrophilic environment, and that the fluorescence changes of the N → I transition are not caused by a single Trp residue but are due to rather global structural changes that affect multiple indole side chains of the proteins simultaneously.

The second unfolding transition (I → U, midpoints at 2.2, 1.8, and 1.5 M GdnHCl for Mi-CK, M-CK, and ArgK, respectively) is less cooperative than the first one; it is accompanied by a further large red shift of the fluorescence emission maximum to 350−352 nm (Figure 1A), which is characteristic for the fully exposed indole fluorophore

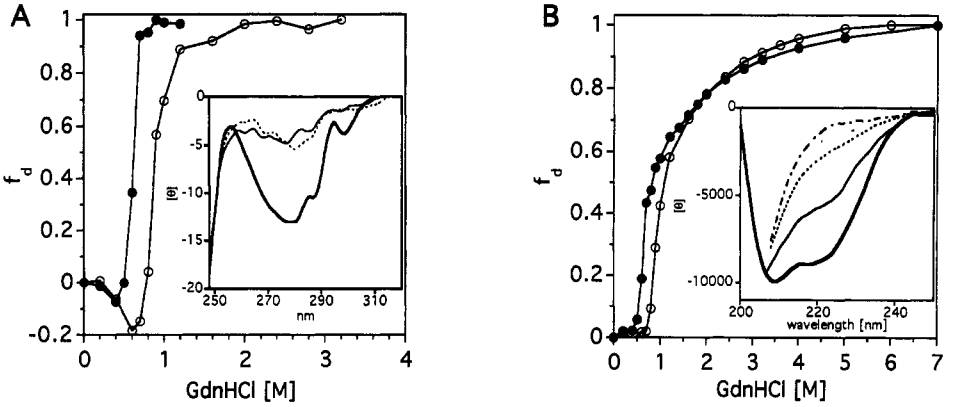

FIGURE 2: Changes in circular dichroism. (A) Near-UV CD unfolding curves of M-CK, ●, and Mi-CK, ○. The proteins were denatured at a concentration of 0.5 mg/mL overnight (22 °C) in buffer A containing the indicated GdnHCl concentrations and measured at a fixed wavelength of 280 nm (bandwidth 2 nm). A total of 10−20 measurements of 8 s each were accumulated. Inset: near-UV CD spectra of native Mi-CK in buffer A, heavy line, and of Mi-CK samples denatured at 1.0, —, and 5.0 M GdnHCl - - -, in buffer A (f_d, fractional signal change). (B) Far-UV CD unfolding profiles of M-CK, ●, and Mi-CK, ○ [same samples as in (A)]. A total of 10 measurements at 222 nm of 8 s each were accumulated. Inset: far-UV CD spectra of native Mi-CK in buffer A, heavy line, and of Mi-CK samples denatured at 1.0, —, 3.0, - - -, and 5.0 M GdnHCl in buffer A, — • — (f_d, fractional signal change). Solubilty problems at the required protein concentrations precluded a similar CD analysis of ArgK.

(Burstein et al., 1973); upon GdnHCl-induced unfolding, the fluorescence quantum yield decreased during this second denaturation step (Figure 1B). In addition, a small emission peak at about 300 nm appeared in the U state, suggesting that Tyr → Trp fluorescence energy transfer became at least partially disrupted. In contrast to the N → I transition, the second denaturation step was not accompanied by a significant change in fluorescence intensity at 380 nm, since the red shift was compensated by the decrease in quantum yield; therefore, fluorescence intensity at 380 nm could be used to follow the N → I transition separately (not shown).

With urea as the denaturant, a similar biphasic unfolding profile was obtained for Mi-CK (Figure 1A; the other proteins were not assayed). Compared to the GdnHCl-induced denaturation, higher denaturant concentrations were required for the two transitions (midpoints for Mi-CK at 2.6 and 4.1 M urea), which were smoother and more overlapping than with GdnHCl.

Circular Dichroism. The effects of increasing GdnHCl concentrations on the tertiary and secondary structures of Mi-CK and M-CK were studied by measuring CD spectra in the near-UV (Figure 2A) and far-UV regions (Figure 2B), respectively. The characteristic pattern of negative bands in the near-UV (Figure 2A, inset), caused by the asymmetric environment of Tyr and Trp residues in the native structure (Oriol & Landon, 1970; Gross et al., 1994; Mühlebach et al., 1994), disappeared simultaneously with the fluorescence−spectroscopic N → I transition (Figure 2A), indicating a significant disruption of the native tertiary structure. In particular, the band centered at 298 nm, which is caused by Trp-206 in native Mi-CK (Gross et al., 1994), is abolished in the I state. Prior to the N → I transition, near-UV CD was slightly enhanced for both Mi-CK and M-CK; this was paralleled by a slight octamer stabilization in the case of Mi-CK (not shown) and is likely to be due to the stabilizing salt effect that is sometimes exerted by low GdnHCl concentrations (Mayr & Schmidt, 1993). In the far-UV range (Figure 2B), the CD amplitude for Mi-CK and M-CK sharply decreased with the N → I transition as well; however, at the end point of the fluorescence−spectroscopic N → I transition, it was only reduced by about 40% (at 222 nm), suggesting a significant retainment of native secondary structure elements in the I state. Far-UV ellipticity continued to decrease steeply immediately after the N → I transition, leveling off to less than 10% of the native ellipticity at 7 M GdnHCl. In contrast to the cooperative I → U transition observed by protein fluorescence, the decrease in far-UV ellipticity beyond the I state was nonsigmoidal for both Mi-CK and M-CK and did not coincide with the fluorescence changes. This suggests that the transition from the I to the U state might involve more unfolding steps than the one cooperative change that is seen by protein fluorescence.

Enzyme Activity. For all three guanidino kinases, the N → I transition was accompanied by a complete loss of enzyme activity (Figure 3A); the changes in enzyme activity were highly cooperative and coincided with the alterations in protein fluorescence.

Hydrophobic Surface Exposure. The hydrophobic fluorescent dye ANS was used to probe Mi-CK, M-CK, and ArgK for the exposure of hydrophobic surface area during GdnHCl-induced equilibrium unfolding. We observed an enhancement of ANS fluorescence in the presence of native CK or ArgK as has been reported earlier (McLaughlin, 1974) and which is due to the binding of the dye to the enzymes' active sites. During the N → I transition, a steep increase in ANS fluorescence enhancement (5−6-fold for CK and 2.5-fold for ArgK; Figure 3B), together with a blue shift of ANS fluorescence (not shown), was observed for all three guanidino kinases. ANS adsorption was most pronounced for ArgK, both in the native state and in the unfolding intermediate, suggesting a larger accessible hydrophobic surface area for this protein compared to the CKs. After a sharp maximum, ANS fluorescence enhancement steeply declined again with increasing GdnHCl concentrations, indicating that the unfolding intermediate of the guanidino kinases exhibits markedly enhanced surface hydrophobicity compared to both the native and the fully unfolded state. Notably, the steep decrease in ANS binding occurred clearly before the second transition seen by protein fluorescence.

Molecular Weight and Hydrodynamic Properties of Denaturation Intermediates. To assess the hydrodynamic radii of the proteins during successive denaturation, SEC-FPLC runs on a Superose-12 column were performed with the denaturation buffers, containing the respective equilibrium concentrations of denaturant, as the eluent ("equilibrium SEC-FPLC"). The unfolding of a single guanidino kinase

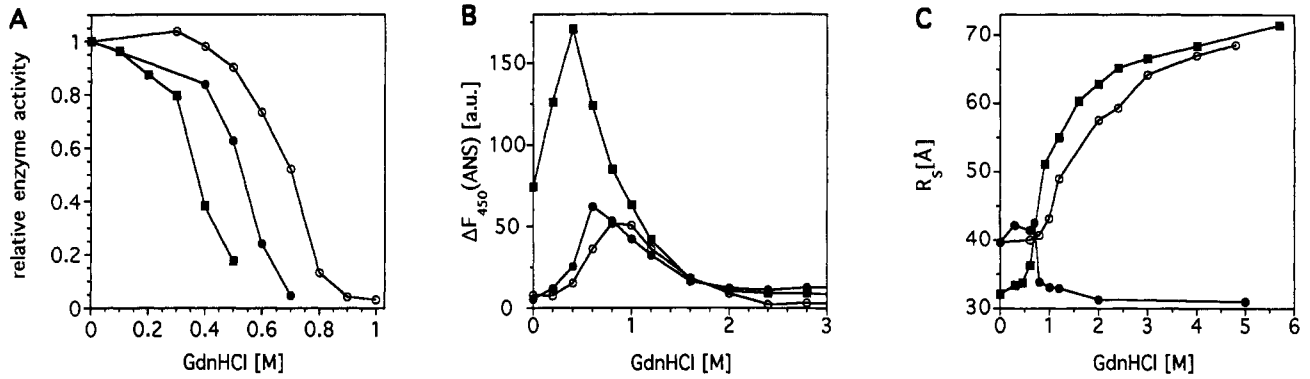

FIGURE 3: Changes in enzyme activity, hydrophobic surface exposure, and molecular size. (A) GdnHCl-dependent inactivation of Mi-CK, ○, M-CK, ●, and ArgK, ■. The proteins were incubated at increasing GdnHCl concentrations in buffer A under conditions as described for Figure 1. Enzyme activities are expressed relative to the activities of identically treated, denaturant-free samples. (B) Enhancement of ANS fluorescence by denatured samples of Mi-CK, ○, M-CK, ●, and ArgK, ■. Equilibrium unfolding was performed as described for Figure 1, followed by incubation of the samples with a 50-fold molar excess of ANS for 30 min at 22 °C. ANS fluorescence was excited at 350 nm and emission intensity measured at 450 nm. The ANS fluorescence of a protein-free blank was subtracted for each sample and the resulting protein-dependent fluorescence enhancement (au, arbitrary units) plotted against GdnHCl concentration. (C) Denaturant-induced changes in Stokes radius of Mi-CK and ArgK. Samples were incubated for ≥3 days at 22 °C in buffer A containing 50 mM 2-ME and the indicated concentrations of GdnHCl. Mi-CK, ○, and ArgK, ■, were run on the SEC-FPLC column at the respective equilibrium GdnHCl concentrations (equilibrium SEC-FPLC). Aliquots of the Mi-CK samples, ● (globularized SEC-FPLC) were diluted into buffer A to a final GdnHCl concentration of 0.3 M (final protein concentration, ≤40 μg/mL) and immediately run on the SEC-FPLC column equilibrated in buffer A containing 0.3 M GdnHCl.

Table 1: Fluorescence-Derived Thermodynamic Denaturation Parameters for Mi-CK, M-CK, and ArgK[a]

	Mi-CK (GdnHCl)	Mi-CK (urea)	M-CK (GdnHCl)	ArgK (GdnHCl)
$\Delta G_{0,ni}$[b]	22.3 ± 2.6	37.6 ± 2.2	18.7 ± 0.9	15.8 ± 8.7
$\Delta G_{0,iu}$[b]	9.3 ± 1.1	9.2 ± 0.2	10.3 ± 0.6	9.2 ± 2.3
$\Delta G_{0,nu}$[b,c]	31.6	46.8	29.0	25.0
m_{ni}[d]	32.3	14.6	32.5	39.0
m_{iu}[d]	4.25	2.46	5.81	6.25
α_{ni}[e]	0.53	0.47	0.52	0.40
$D_{50,ni}$ (M); $D_{50,iu}$ (M)[f]	0.69; 2.18	2.58; 4.10	0.57; 1.77	0.40; 1.47
f_I^{max}; D_I^{max} (M)[g]	0.87; 1.00 M	0.61; 3.10 M	0.87; 0.90 M	0.87; 0.65 M

[a] The data were obtained by fitting of the biphasic ⟨λ⟩ curves (Figure 1A) to a unimolecular three-state denaturation model (see Materials and Methods). A representative deconvolution is shown in Figure 4. [b] Kilojoules per mole. [c] Sum of $\Delta G_{0,ni}$ and $\Delta G_{0,iu}$. [d] Cooperativity index of the transition, (in kJ L mol^{-2}). [e] Calculated fractional contribution of the N → I transition to the total signal change. [f] Calculated denaturant concentration at transition midpoint. [g] Calculated maximum fraction of intermediate I and corresponding denaturant concentration.

protomer can be seen best in the equilibrium SEC-FPLC profile of ArgK (Figure 3C), which is already monomeric in the native state. The native protein displays a Stokes radius of about 32 Å, as determined by calibration of the Superose column with globular reference proteins. At 0.45 M GdnHCl, which is beyond the midpoint of the fluorescence–spectroscopic N → I transition (see Table 1 and Figure 1), the protein appears to be swollen by only about 10%; the main, steep increase in size, however, occurs only *after* the N → I transition. In the fully unfolded state, the Stokes radius of ArgK is more than doubled with respect to the native protein. For Mi-CK (Figure 3C), the interpretation of the equilibrium SEC-FPLC profile is more complicated, since both subunit dissociation (reduction in size) and unfolding steps (increase in size) contribute to the observed overall changes. The SEC-FPLC elution profiles clearly indicated that the Mi-CK octamers dissociate into dimers prior to the fluorescence–spectroscopic N → I transition (not shown); therefore, the octamer–dimer equilibrium does not interfere with unfolding. Beyond 0.8 M GdnHCl, where the dimers were completely dissociated into monomers (see below), the equilibrium SEC-FPLC unfolding profile for Mi-CK was very similar to the one for ArgK, except for a shift of the transitions toward higher denaturant concentrations.

A second type of gel permeation experiments ("globularized SEC-FPLC") was used to monitor the subunit dissociation of CK directly. For this, the denatured samples were diluted to a uniform GdnHCl concentration of 0.3 M prior to running them on the Superose-12 column at 0.3 M GdnHCl. We found that, within the dead time of the experiment, the proteins folded back into a compact, globular structure; however, at the dilute conditions used (see Materials and Methods), no significant reassociation of CK dimers took place. This method was therefore used to determine the point of dimer dissociation for Mi-CK. The globularized SEC-FPLC experiments with Mi-CK (Figure 3C) clearly revealed that dissociation into monomers occurs between 0.7 and 0.8 M GdnHCl, indicating that the fluorescence–spectroscopic N → I transition and subunit dissociation are simultaneous events. The Stokes radius of the "reglobularized" Mi-CK sharply changed from 42 Å to smaller than 34 Å beyond 0.7 M GdnHCl; this latter value is close to the size of native ArgK (see above). This confirms that denatured, monomeric Mi-CK indeed folds back rapidly into a nativelike, globular structure upon dilution of the denaturant.

Sedimentation equilibrium and velocity experiments, respectively, were used to determine the molecular weights and sedimentation coefficients for Mi-CK in the presence of 1, 3, and 5 M GdnHCl. The data support the results obtained by SEC-FPLC, showing that Mi-CK (calculated protomer M_r = 43 200) is indeed monomeric at 1 M GdnHCl. An average M_r of 43 000 at 1 M GdnHCl, however, was only observed when fresh DTT (15 mM) had been added to the sample prior to the sedimentation equilibrium runs. In the absence of DTT, average M_r values between 67 000 and 90 000, and clear signs of inhomogeneity were found. In contrast, at 3 and 5 M GdnHCl, no additional reducing agent was required to obtain a solution of apparently homogeneously monomeric Mi-CK, with average molecular weights

of 50 000, and 46 000, respectively. This suggests that, in the I state at high protein concentrations, Mi-CK exhibits a strong tendency to form intermolecular disulfide cross-links, giving rise to covalent high molecular weight aggregates. A sedimentation constant of 3.0 S was determined for the I state of Mi-CK (in the presence of DTT), which is only compatible with a monomeric, globular molecule; for comparison, a compact monomeric GdnHCl unfolding intermediate of aspartate aminotransferase (M_r = 43 500) has been reported to exhibit a sedimentation constant of 3.1 S (Herold & Kirschner, 1990). The $s_{20,w}$ values of 2.4 and 2.1 S that were determined for Mi-CK at 3 and 5 M GdnHCl reflect the further unfolding of the globular protein into an extended, random coil-like structure.

Quantitative Evaluation of Denaturation Parameters. The unfolding of all three guanidino kinases was reversible, as confirmed by the regain of enzyme activity after dilution of the denaturant (not shown); however, the yield of recovered activity (usually 70−80%) dropped significantly when samples treated with intermediate denaturant concentrations were renatured at low concentrations of 2-ME (not shown). We therefore also performed denaturation series at higher 2-ME concentrations (20 and 50 mM, not shown) to assess the influence of the reducing agent on the shape of the unfolding profiles. In such GdnHCl denaturation series, the N → I transition midpoint was slightly shifted (by +0.03 and +0.08 M, respectively) with respect to the standard low-2-ME conditions (5 mM). However, apart from this small shift of the transition midpoint, the shape of the denaturation profiles was not affected by the higher concentration of 2-ME. Since high concentrations of thiol agents interfered with all methods requiring UV detection (fluorescence, CD, analytical ultracentrifugation), we used low-2-ME conditions (5 mM) for our standard experiments; the quantitative parameters derived from these experiments must therefore be considered apparent values that do not reflect a perfect equilibrium state.

The biphasic fluorescence−spectroscopic GdnHCl unfolding curves for Mi-CK, M-CK, and ArgK, as well as the urea denaturation curve for Mi-CK, were analyzed by fitting the data to a three-state denaturation model (eq 3). Although the CKs form oligomers in the native state, all three proteins were treated according to a simple, unimolecular scheme in order to allow for a comparison and to avoid additional complexity of the analysis. The results of the fits to the three-state model are given in Table 1; an exemplary curve fit for M-CK is shown in Figure 4. Reproducible and unambiguous values for the five denaturation parameters, α_{ni}, $\Delta G_{0,ni}$, $\Delta G_{0,iu}$, m_{ni}, and m_{id} were obtained. However, in some cases the experimental data points showed slight deviations from the assumed model. This may be due to (i) direct solvent effects of the denaturants on protein fluorescence, (ii) incomplete reversibility of the first transition, and (iii) the possible occurrence of additional unfolding intermediates (see Discussion). The denaturant effects (i) on protein fluorescence that are not due to unfolding could theoretically be accounted for by introducing baseline terms into the fitting equation; however, in the present case, this requires the addition of six fitting parameters (i.e., the intercepts and slopes for the baseline effects in the native, intermediate, and unfolded states, respectively), which would produce ambiguous results. Therefore, due to the complexity of the system, a baseline correction was not performed, and one must be aware that the obtained values contain some uncertainty.

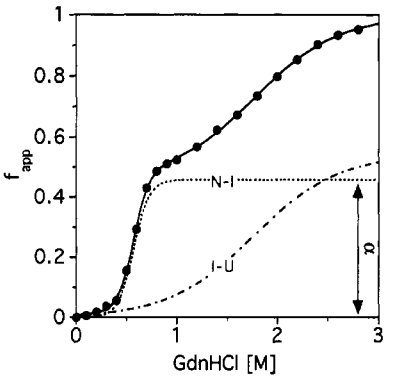

FIGURE 4: Deconvolution of an exemplary fluorescence-derived unfolding profile. The experimental GdnHCl equilibrium unfolding profile of M-CK, ●, measured by intrinsic protein fluorescence (see Figure 1A), was fit to a three-state model, —, as described in Materials and Methods. From the optimized fitting parameters (values given in Table 1), the fractional contributions of the fluorescence−spectroscopic N → I, - - -, and I → U transition, — • —, to the total signal change were calculated.

The overall conformational stability of the three proteins is reflected by the $\Delta G_{0,nu}$ values (Table 1). They decrease in the order Mi-CK (32 kJ/mol) > M-CK (29 kJ/mol) > ArgK (25 kJ/mol). The $\Delta G_{0,ni}$ values for Mi-CK, derived from GdnHCl and urea denaturation, respectively, differed significantly from each other. Such discrepancies are commonly encountered when GdnHCl and urea data are compared (Pace, 1986); however, there was no significant difference between the urea- and GdnHCl-derived parameters for the second unfolding transition of Mi-CK. The I state for all proteins appeared to be energetically closer to the fully denatured than to the native state, since the $\Delta G_{0,iu}$ values were always significantly smaller than the $\Delta G_{0,ni}$. Also, the cooperativity of the second transition seemed to be generally lower compared to the first denaturation step. The individual transition midpoints, recalculated from the thermodynamic parameters, agreed very well with the directly observed midpoints (the midpoints of the second transition, which were not well defined in plots of $\langle\lambda\rangle$, can be independently determined from λ_{max} curves; see Figure 1A). The populations of the I state could be estimated using the obtained ΔG_0 and m values; the results of such calculations suggest that the I state is maximally populated to about 87% at the respective optimum GdnHCl concentrations (Table 1). When urea is used for denaturation, only an I state population of 61% can theoretically be achieved. These results suggest that, by choosing appropriate GdnHCl concentrations, highly enriched I state populations can be obtained for all guanidino kinases, rendering this type of unfolding intermediate well suited for a biophysical and biochemical characterization.

DISCUSSION

Occurrence of a Stable Unfolding Intermediate. The fluorescence−spectroscopic equilibrium unfolding profiles of the three guanidino kinases Mi-CK, M-CK, and ArgK exhibited a pronouncedly biphasic shape (Figure 1A), indicating the occurrence of a stable unfolding intermediate. The first, highly cooperative unfolding transition was characterized by a strong red shift of the fluorescence emission maximum to a uniform value of about 340 nm (shown for Mi-CK in Figure 1A). It was accompanied by a

complete loss of enzyme activity (Figure 3A), subunit dissociation (for the CKs; Figure 3C), an abolishment of the native near-UV CD characteristics (Figure 2A), a 40% reduction of native far-UV ellipticity (Figure 2B), and a steep increase of hydrophobic surface area (Figure 3B). The second fluorescence−spectroscopic transition included a further red shift of fluorescence emission (Figure 1), a progressive decline of far-UV ellipticity (Figure 2B), and a large expansion of hydrodynamic radius (Figure 3C). Despite their different quaternary structures in the native state (Mi-CK, octameric; M-CK, dimeric; ArgK, monomeric), all three guanidino kinases exhibited such biphasic unfolding transitions. This suggests that the specific oligomeric interactions of the CKs are not involved in stabilizing the intermediate state but that the occurrence of the equilibrium unfolding intermediate might rather be a common intrinsic feature of the guanidino kinase protomers.

The biophysical and biochemical features of the fluorescence−spectroscopically observed I state of the guanidino kinases are formally consistent with the definition of the "molten globule", a type of unfolding intermediate that is characterized by a retainment of globular shape and a high conservation of native secondary structure, whereas native tertiary structure interactions are largely abolished (Kuwajima, 1989). However, the observed properties of the I state may alternatively be explained by a sequential unfolding of at least two structural domains of the guanidino kinases. In particular, the high capacity for ANS binding in the I state might be attributed to the exposure of a hydrophobic domain interface upon the denaturant-induced detachment and/or unfolding of the first domain.

A pronounced exposure of hydrophobic surface area in the I state could also be a reason for the strong tendency of the intermediates to form intermolecular disulfide bonds, as suggested by analytical ultracentrifugation in the presence and absence of freshly added DTT.

Energetics of Unfolding and Influence of Quaternary Structure. A quantitative evaluation of the biphasic fluorescence unfolding profiles (Table 1) revealed a decreasing total conformational stability for the three enzymes in the order Mi-CK > M-CK > ArgK. For all three proteins, the calculated free energy of the I → U transition was about the same, suggesting that, on a rather fundamental structural level, which could possibly be defined by the hydrophobic core, these enzymes are closely related. In contrast, the free energies of the N → I transition differed significantly among the three enzymes, indicating substantial differences in structural stability on a level of weaker interactions. The position of the N → I transition for M-CK was independent of protein concentration within the range of 0.025−0.5 mg/mL (not shown), suggesting a submicromolar dissociation constant of the CK dimers. This agrees well with the fact that wild-type CK dimers do not dissociate under nondenaturing conditions. The thermodynamic linkage of dimer dissociation to the unfolding process suggests that at least part of the additional conformational stability of the CKs compared to ArgK should be due to monomer−monomer interaction energy. On the other hand, the octameric structure of Mi-CK was found to dissociate into dimers clearly prior to the N → I transition; in fact, octamer formation is readily reversible under native conditions (Schlegel et al., 1988; Gross & Wallimann, 1993, 1995). Therefore, the contribution of dimer−dimer contacts to folding stability is likely to be much smaller compared to the monomer−monomer interactions.

Possible Occurrence of Additional Unfolding Intermediates. Several biophysical parameters of the guanidino kinases changed sharply in a range of denaturant concentrations where no significant alterations of protein fluorescence occurred, i.e., *between* the fluorescence−spectroscopic N → I and I → U transitions. Such changes included a significant decrease in far-UV ellipticity (Figure 2B), the steepest phase of the increase in Stokes radius (Figure 3C), and a sharp decrease in ANS binding (Figure 3B). This suggests that there may be additional unfolding transitions that are not "sensed" by the proteins' Trp residues. In fact, all Trp residues of the guanidino kinases are clustered within a stretch of 63 amino acids within the C-terminal half of the protein sequences (Gross et al., 1994; Mühlebach et al., 1994), suggesting that the strong changes in protein fluorescence might mainly reflect conformational alterations within a structural moiety comprising these residues, whereas the fluorescence-invisible unfolding transitions might rather correspond to changes in regions distinct from this C-terminal part. Indeed, there is strong evidence that the guanidino kinases are flexibly-hinged two-domain enzymes (Dumas & Janin, 1983), such as 3-phosphoglycerate kinase (Watson et al., 1982). Therefore, it is possible that the observed unfolding profiles reveal an independent unfolding of the putative N-terminal and C-terminal domains, with the fluorescence-silent transitions reflecting the unfolding of the Trp-free N-terminal domain. Near-UV ellipticity (Figure 2A) parallels the fluorescence−spectroscopic N → I transition since, similar to protein fluorescence, the near-UV CD pattern of the guanidino kinases probably originates mainly from aromatic residues of the C-terminal domain (Gross et al., 1994).

The results presented here, however, do not yet allow one to construct a clear-cut two-domain unfolding pathway of the guanidino kinases, since the data would be consistent with several alternative unfolding models. In particular, the folding state of the individual domains within the equilibrium intermediate has to be further characterized. To approach this problem, we are currently performing small-angle X-ray scattering experiments; furthermore, denaturation experiments with isolated Mi-CK fragments corresponding to the two expected domains are under way, hopefully leading to an assignment of the observed unfolding transitions to the corresponding domains.

Literature Data and Relevance of Equilibrium Intermediates to the Folding Process. The data presented here on the denaturant-induced inactivation of CK significantly differ from results reported previously (Yao et al., 1984; Zhou et al., 1993). In contrast to the present study, Zhou et al. generally measured CK enzyme activities in the presence of the respective denaturant concentrations used for unfolding, resulting in a fast, apparently noncooperative inactivation that did not coincide with any other changes in intrinsic properties. However, this inactivation was paralleled by a decrease in fluorescence anisotropy of a covalently bound OPTA label, which was interpreted to reflect a local unfolding of the enzyme's active site. In contrast to that, we never observed any red shift of protein fluorescence at low denaturant concentrations, which should be expected upon exposure of the active-site Trp residue (Vasak et al., 1979; Zhou & Tsou, 1985; Gross et al., 1994) in case of a local denaturation. We would therefore rather argue that low

concentrations of denaturant have an *inhibitory* effect on CK, such that the inactivation curves obtained by Zhou et al. represent a sum of inhibitory and "true" denaturation effects, and that the observed decrease in OPTA fluorescence anisotropy might rather be due to fluorescence lifetime changes of the probe than to an increased flexibility at the active site. It might, however, be a matter of definition of what should be termed "inhibition" or "denaturation". We therefore decided to monitor only the slow and slowly reversible inactivation that was observed by measuring enzyme activities at low, uniform residual denaturant concentrations and that coincided with fluorescence and other changes. In a recent paper (Grossman, 1994), a third variation of measuring the GdnHCl-induced inactivation of M-CK was presented. There, the denatured protein was added to a denaturant-free assay mix without equalizing the residual GdnHCl concentrations. The resulting, apparently biphasic inactivation curves clearly represent a combination of both inhibitory and denaturing GdnHCl effects.

Earlier studies on the unfolding and refolding of CK by Grossman et al. (1981) showed that the minimal urea concentration required to produce MB-CK heterodimers out of homodimeric M- and B-CK was 2 M; this perfectly coincides with the onset of our fluorescence–spectroscopically observed N → I transition, which we found to be accompanied by monomerization. Upon renaturation of fully denatured CK, Grossman's group (Grossman, 1984; Grossman et al., 1986) observed very fast initial changes in protein fluorescence, occurring within the dead time of a standard fluorescence spectrometer. In preliminary experiments, we found that the fluorescence spectra of Mi-CK renatured for ≤10 s were very similar to the ones of the equilibrium intermediate at 1 M GdnHCl, showing an emission maximum at 340 nm (not shown). These findings are likely to reflect the fast formation ("hydrophobic collapse") of a globular folding intermediate with properties similar to the equilibrium I state; this assumption is further corroborated by the rapid formation of a compact structure as observed by SEC-FPLC (Figure 3C). Fast-forming, globular folding intermediates have been reported in many other cases, such as for bovine carbonic anhydrase, human α-lactalbumin, and yeast 3-phosphoglycerate kinase (3-PGK) (Ptitsyn et al., 1990). In analogy to the unfolding behavior shown here for the guanidino kinases, the equilibrium unfolding of 3-PGK, also being a "two-substrate/two-domain" enzyme (Watson et al., 1982) was reported to involve both "hierarchic" (including MG-like intermediates) and "sequential" (i.e., the independent unfolding of individual domains) unfolding events (Betton et al., 1989; Mitraki et al., 1987; Missiakas et al., 1990; Griko et al., 1989). Hence, we would like to speculate that the formation of both equilibrium and kinetic globular folding intermediates might be a general feature inherent in the common structure type of guanidino kinases, and that this might apply to other related kinases as well.

ACKNOWLEDGMENT

We thank Dr. Elizabeth Furter-Graves for carefully revising the manuscript. The group of Prof. K. Wüthrich (ETH Institute for Molecular Biology and Biophysics) is gratefully acknowledged for kindly providing the fluorescence and CD spectroscopic instrumentation.

REFERENCES

Betton, J.-M., Desmadril, M., & Yon, J. M. (1989) *Biochemistry 28*, 5421–5428.
Bickerstaff, G. F., Paterson, C., & Price, N. C. (1980) *Biochim. Biophys. Acta 621*, 305–314.
Bradford, M. M. (1976) *Anal. Biochem. 72*, 248–254.
Burstein, E. A., Vedenkina, N. S., & Ivkova, M. N. (1973) *Photochem. Photobiol. 18*, 263–279.
Cantor, C. R., & Schimmel, P. R. (1980) *Biophysical Chemistry Part II*, p 626, Freeman & Co., New York.
Dumas, C., & Janin, J. (1983) *FEBS Lett. 153*, 128–130.
Furter, R., Kaldis, P., Furter-Graves, E. M., Schnyder, T., Eppenberger, H. M., & Wallimann, T. (1992) *Biochem. J. 288*, 771–775.
Griko, Y. V., Venyaminov, S. Y., & Privalov, P. L. (1989) *FEBS Lett. 244*, 276–278.
Gross, M., & Wallimann, T. (1993) *Biochemistry 32*, 13933–13940.
Gross, M., & Wallimann, T. (1995) *Biochemistry 34*, 6660–6667.
Gross, M., Furter-Graves, E. M., Wallimann, T., Eppenberger, H. M., & Furter, R. (1994) *Protein Sci. 3*, 1058–1068.
Grossman, S. H. (1984) *Biochim. Biophys. Acta 785*, 61–67.
Grossman, S. H. (1994) *Biochim. Biophys. Acta 1209*, 19–23.
Grossman, S. H., Pyle, J., & Steiner, R. J. (1981) *Biochemistry 20*, 6122–6128.
Grossman, S. H., Gray, K. A., & Lense, G. J. (1986) *Arch. Biochem. Biophys. 248*, 234–242.
Herold, M., & Kirschner, K. (1990) *Biochemistry 29*, 1907–1913.
Kuwajima, K. (1989) *Proteins: Struct. Funct. Genet. 6*, 87–103.
Martin, J., Langer, T., Boteva, R., Schramel, A., Horwich, A. L., & Hartl, F.-U. (1991) *Nature 352*, 36–42.
Mayr, L. M., & Schmidt, F. X. (1993) *Biochemistry 32*, 7994–7998.
McLaughlin, A. C. (1974) *J. Biol. Chem. 249*, 1445–1452.
Missiakas, D., Betton, J.-M., Minard, P., & Yon, J. M. (1990) *Biochemistry 29*, 8683–8689.
Mitraki, A., Betton, J.-M., Desmadril, M., & Yon, J. M. (1987) *Eur. J. Biochem. 163*, 29–34.
Morris, G. E., & Cartwright, A. J. (1990) *Biochim. Biophys. Acta 1039*, 318–322.
Mühlebach, S., Gross, M., Wirz, T., Wallimann, T., Perriard, J. C., & Wyss, M. (1994) *Mol. Cell. Biochem. 133/134*, 245–262.
Oriol, C., & Landon, M.-F. (1970) *Biochim. Biophys. Acta 214*, 455–462.
Pace, C. N. (1986) *Methods Enzymol. 131*, 266–280.
Price, N. C., & Stevens, E. (1982) *Biochem. J. 201*, 171–177.
Ptitsyn, O. B., Pain, R. H., Semisotnov, G. V., Zerovnik, E., & Razgulyaev, O. I. (1990) *FEBS Lett. 262*, 20–24.
Roustan, C., Pradel, L. A., Kassab, R., Fattoum, A., & Thoai, N. V. (1970) *Biochim. Biophys. Acta 206*, 369–379.
Royer, C. A., Mann, C. J., & Matthews, C. R. (1993) *Protein Sci. 2*, 1844–1852.
Schlegel, J., Zurbriggen, B., Wegmann, G., Wyss, M., Eppenberger, H. M., & Wallimann, T. (1988) *J. Biol. Chem. 263*, 16942–16953.
Vasak, M., Nagayama, K., Wüthrich, K., Mertens, M., & Kägi, J. H. R. (1979) *Biochemistry 18*, 5050–5055.
Wallimann, T., Schlösser, T., & Eppenberger, H. M. (1984) *J. Biol. Chem. 259*, 5238–5246.
Watson, H. C., Walker, N. P. C., Shaw, P. J., Bryant, T. N., Wendell, P. L., Fothergill, L. A., Perkins, R. E., Conroy, S. C., Dobson, M. J., Tuite, M. F., Kingsman, A. J., & Kingsman, S. M. (1982) *EMBO J. 1*, 1635–1640.
Yao, Q.-Z., Tian, M., & Tsou, C.-L. (1984) *Biochemistry 23*, 2740–2744.
Zhou, H.-M., & Tsou, C.-L. (1985) *Biochim. Biophys. Acta 830*, 59–63.
Zhou, H.-M., Zhang, X.-H., Yin, Y., & Tsou, C. L. (1993) *Biochem. J. 291*, 103–107.

BI950554S